Chemical Science

ROYAL SOCIETY OF CHEMISTRY

EDGE ARTICLE

View Article Online
View Journal | View Issue

Cite this: *Chem. Sci.*, 2024, **15**, 3182

All publication charges for this article have been paid for by the Royal Society of Chemistry

Received 25th October 2023
Accepted 20th December 2023

DOI: 10.1039/d3sc05700c

rsc.li/chemical-science

Strain-enabled radical spirocyclization cascades: rapid access to spirocyclobutyl lactones and – lactams†

Kousik Das, Abhilash Pedada, Tushar Singha and Durga Prasad Hari *

Spirocyclobutane derivatives have gained significant attention in drug discovery programs due to their broad spectrum of biological activities and clinical applications. Ring-strain in organic molecules is a powerful tool to promote reactivity by releasing strain energy, allowing the construction of complex molecules selectively and efficiently. Herein, we report the first strain-enabled radical spirocyclization cascades for the synthesis of functionalized spirocyclobutyl lactones and – lactams, which are finding increasing applications in medicinal chemistry. The reaction of interelement compounds with bicyclobutane (BCB) allyl esters and – amides proceeds with high chemoselectivity under simple, catalyst-free conditions using blue light irradiation. The reaction has been successfully extended to synthesize bis-spirocycles. To introduce a more diverse set of functional groups, we have developed a dual photoredox/nickel catalytic system capable of mediating the carbosulfonylation of BCB allyl amides. The reaction shows broad applicability across various (hetero)aryl halides, aryl sulfinates, and BCB allyl amides, operates under mild conditions and demonstrates excellent functional group compatibility. The functional groups introduced during the cascade reactions served as versatile handles for further synthetic elaboration.

Introduction

Spirocyclic compounds are among the most important structural components of small-molecule drug candidates.[1] Due to their rigid conformation, substituents on spirocyclic scaffolds are well-defined in their spatial arrangement and, thus, allow for the orientation of various functional groups along the designated vectors. As a result, interactions of a ligand with a three-dimensional (3D) binding site can be attained more effectively with a spirocyclic motif than with flat aromatic compounds.[2] Owing to its unique puckered structure, the inclusion of a cyclobutane ring also allows for the orientation of substituents along pre-selected vectors, and it improves certain physicochemical properties and pharmacokinetics, such as metabolic stability, lipophilicity, and acidity/basicity (Scheme 1A).[3] All these factors have fueled a rush in reports of biologically active spirocyclobutane-based compounds.[1c,4] Among these, spirocyclobutyl lactones and – lactams have gained significant attention in medicinal chemistry discovery programs due to their broad biological activity spectrum (Scheme 1A).[5] Despite this, there is scant literature on the synthesis of these privileged motifs.[6] Another limitation is the difficulty in accessing functionalized spirocyclobutyl lactones and – lactams that would allow extra structural variations. Such motifs would represent very useful building blocks that could foster the application of these spirocycles in drug discovery.[5]

Strain energy in organic molecules is a powerful driving force that promotes reactivity through the release of ring-strain, allowing a plethora of valuable transformations with applications in various research fields, including total synthesis, bioconjugation, bioisosterism, and polymer science.[7] Bicyclobutane (BCB), the smallest fused strained hydrocarbon with a ring-strain of 64 kcal mol^{-1}, gained significant attention in recent years not only due to its unique structural features but also its ability to unlock strategies through strain release to synthetically challenging compounds either *via* single-electron or two-electron pathways.[8] For example, the stained carbon–carbon bond of BCB derivatives participates in various difunctionalization,[6c,9] carbene insertion,[10] or cycloaddition reactions,[11] leading to highly valuable carbocycles and heterocycles, which are bioisosteres of (hetero)arenes (Scheme 1B).[12] Despite the growing number of synthetic strategies using BCBs, reports on strain-enabled radical spirocyclization cascades haven't been studied to date. However, such radical strategies would give rapid access to functionalized spirocyclobutane derivatives, which are finding increasing applications in pharmaceuticals.[5]

Fundamentally new triggers for spirocyclization, especially for the construction of all-carbon quaternary spirocentres, are

Department of Organic Chemistry, Indian Institute of Science, Bangalore, India, 560012. E-mail: dphari@iisc.ac.in

† Electronic supplementary information (ESI) available. CCDC 2259733 and 2292233. For ESI and crystallographic data in CIF or other electronic format see DOI: https://doi.org/10.1039/d3sc05700c

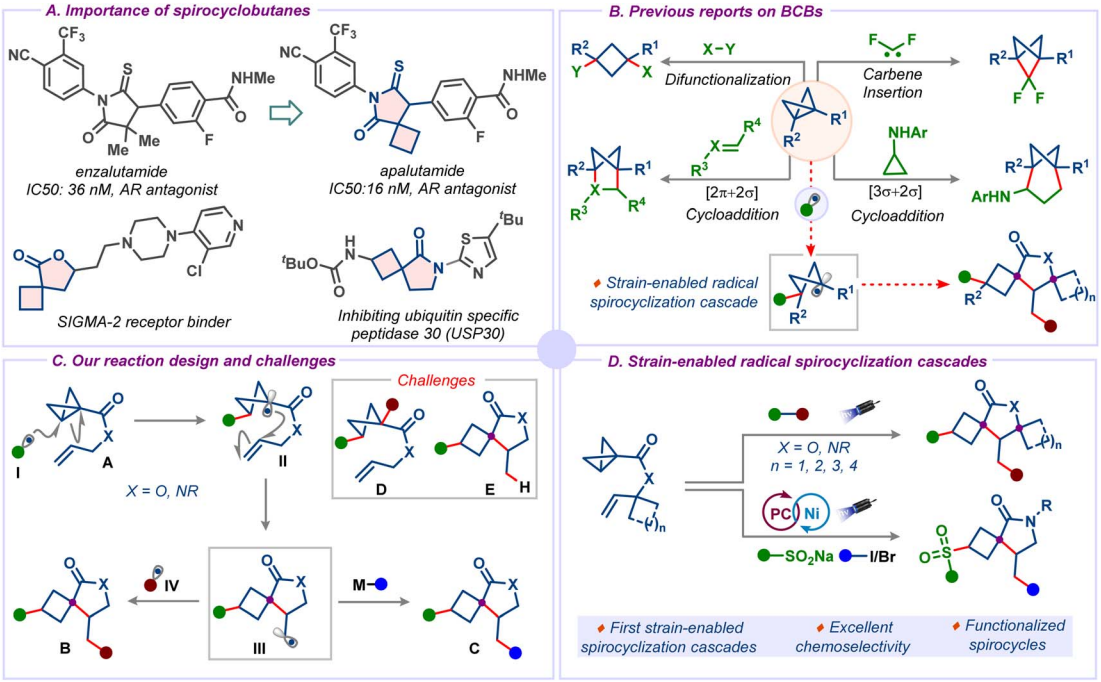

Scheme 1 (A) Importance of spirocyclobutanes. (B) Previous reports on BCBs. (C) Our reaction design and challenges. (D) This work: strain-enabled radical spirocyclization cascades.

highly desirable since they have the potential to open considerable chemical space and can lead to new avenues in chemical synthesis. We envisioned the possibility of a novel strain-enabled radical spirocyclization cascade. This approach involves a series of well-orchestrated, radical-mediated bond-forming events (Scheme 1C). We hypothesized that radical intermediate **II** could be accessed by the addition of radical **I**, which could be generated either by photolysis or single electron oxidation of the corresponding radical precursor, onto the strained carbon–carbon bond of BCB **A**. Subsequent 5-*exo*-trig cyclization would lead to alkyl radical **III** that could be trapped with another radical intermediate **IV** to give spirocyclobutane **B**. Alternatively, the radical **III** could also be intercepted with a metal species under metallophotoredox catalysis for further functionalization to afford spirocyclobutane **C**. We recognized three main challenges associated with the successful realization of this radical cascade: (1) the radical **I** should first add chemoselectively to the strained carbon–carbon bond rather than adding to the π bond of the olefin, (2) the rate of cyclization of the radical intermediate **II** should be faster than the direct functionalization to avoid the direct addition product **D**, and (3) the further functionalization of alkyl radical **III** should be quicker to prevent the formation of hydrogen atom transfer (HAT) product **E** (Scheme 1C). Notwithstanding these challenges, here we describe the successful realization of this strategy and report the first strain-enabled radical spirocyclization cascades, providing rapid access to functionalized spirocyclobutyl lactones and – lactams for augmenting medicinal chemistry libraries (Scheme 1D). Notably, the methodology was employed to access bis-spirocycles, which constitute the core frameworks of bioactive compounds.[13] To broaden the scope, we have developed a dual photoredox/nickel catalytic system capable of mediating the carbosulfonylation of BCB allyl amides. The mild conditions display excellent functional group tolerance and broad substrate scope. Furthermore, the functional groups introduced during the reaction served as versatile handles for further synthetic modifications.

Results and discussion

Initial exploration into the proposed spirocyclization cascade process focused on using BCB tethered allyl ester **1a** and a bifunctional oxime ester **4**, which was previously used by Glorius and co-workers for difunctionalization of alkenes under energy transfer photocatalysis (Scheme 2).[14] When we irradiated a mixture of **1a** and **4** using thioxanthone as a photocatalyst in EtOAc, the formation of desired spirocycle **5** was not observed and the starting material BCB was simply reisolated. Next, we used molecular iodine under light irradiation to promote the cascade.[15] Although we didn't detect the desired spirocycle, the direct di-iodination product **6** was formed in 43% yield.[16] Our attempts to cyclize **6** under photochemical conditions were unsuccessful. To force the cyclization, we sought to use the Thorpe–Ingold effect[17] by employing the *gem*-dimethyl substituted BCB allyl ester **1b**. However, treatment of **1b** with iodine also delivered the di-iodination product **7** instead of the spirocycle product. Next, we turned our attention to employing diphenyl disulfide **2a**, which is known to add to unsaturated compounds and strained carbon–carbon bonds and can also capture carbon radicals.[18]

To our delight, the treatment of **1b** with diphenyl disulfide **2a** under blue light irradiation delivered the desired spirocycle **3a**

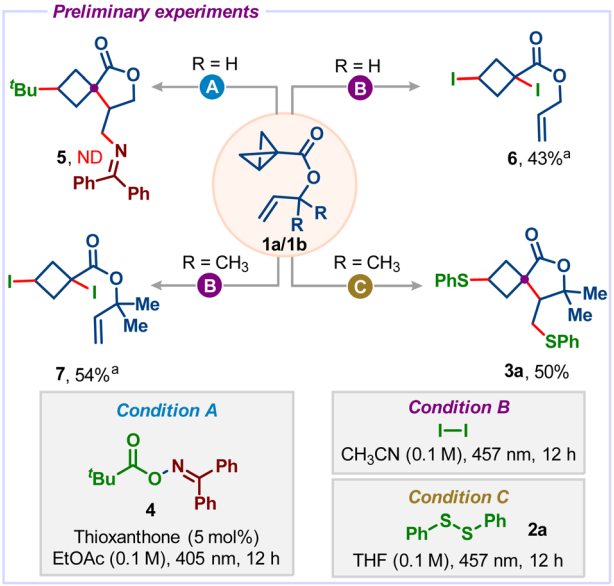

Scheme 2 Preliminary experiments. [a] Direct iodine addition products were also obtained without light irradiation. We used light irradiation to cyclize it, but unfortunately, it didn't work.

in 50% yield along with the direct addition product **8** and HAT product **9**. These initial results encouraged us to optimize this reaction further. Among the solvents tested (Fig. 1, columns 1–6): CH_3CN was the optimal solvent, suppressing the formation of undesired products **8** and **9** and furnishing the desired product in 77% yield. When the reaction was performed using the Ir-photocatalyst, which was employed for transferring the energy to dialkyl disulfide,[18a] no reaction was observed (Fig. 1, column 7). A control experiment demonstrated the importance of light, as **3a** was not observed in the dark, even at 60 °C (Fig. 1, column 8).

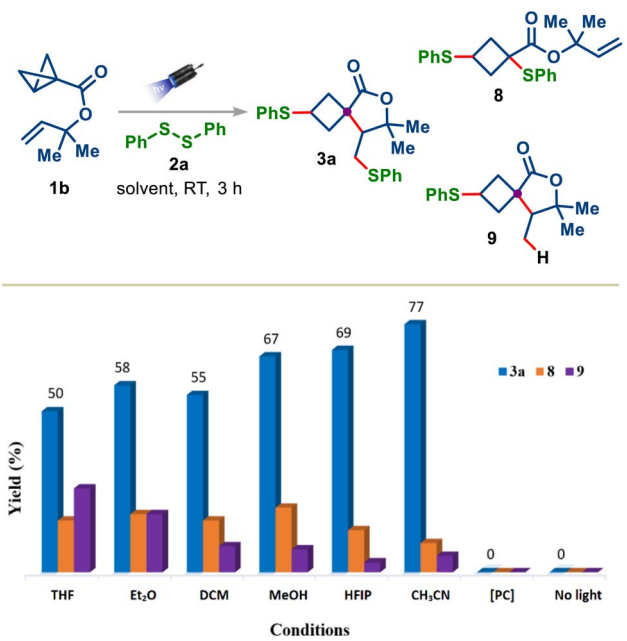

Fig. 1 Optimization of the reaction conditions. Reactions were carried out under an inert atmosphere. Conditions: **1b** (0.15 mmol), **2a** (0.15 mmol), solvent (1.5 mL, 0.1 M), 457 nm photocube, 3 h. [PC] = $[Ir(dF(CF_3)ppy)_2(dtbbpy)]PF_6$. Yields were determined by ^{1}H-NMR using CH_2Br_2 as the internal standard. Depending on the solvent, dr varied between 1.7 : 1 to 1.2 : 1 (see the ESI†).

Having established the optimal conditions, the scope of BCB allyl esters was evaluated using 1,2-bis(4-methoxyphenyl) disulfane (**2b**) (Scheme 3). Simple *gem*-dimethyl substituted BCB allyl ester **1b** provided the spirocycle **3b** in 75% yield. Next, we applied our methodology for the synthesis of bis-spirocyclic scaffolds, which are core frameworks in several biologically active natural products and show attractive features, including high three-dimensional character, molecular complexity, and rich Fsp^3.[13] To our delight, the reaction worked efficiently with cyclobutyl, cyclopentyl, cyclohexyl, cycloheptyl, and piperidinyl appended BCB allyl esters, providing the corresponding bis-spirocycles **3c–3g** in moderate to good yields. Subsequently, we explored the scope of the diaryl disulfides using BCB allyl ester **1e**. Simple diphenyl disulfide and electron-donating substituents bearing diaryl disulfides underwent the desired transformation successfully to afford bis-spirocycles **3h–3k**. Notably, 1,2-bis(4-bromophenyl)disulfane also participated well in this reaction, furnishing the desired spirocycle **3j**, leaving the C–Br bond intact, which is useful for further synthetic diversification. The reaction was not limited to BCB allyl esters; a range of BCB allyl amides having different substituents on nitrogen could be used successfully, providing access to spirocyclobutyl lactams in good yields (products **3l–3p**).

Organoselenium compounds are not only present in several bioactive compounds but are also highly valuable synthetic intermediates as they can be efficiently converted into a broad range of useful functional groups.[19] Therefore, next, we turned our attention to accessing selenium-substituted spirocycles. Pleasingly, diphenyl diselenide reacted well under our standard conditions with both BCB allyl esters and – amides, giving the desired spirocycles in moderate to high yields (products **3q–3v**). Notably, selenium appended bis-spirocycles **3w–3y** could also be accessed.

Next, we sought to explore various interelement radical precursors to selectively introduce different functional groups, which can be further functionalized orthogonally. We were pleased to find that the reaction of BCB allyl amide **1l** with *S*-(4-methylphenyl)4-methylbenzenethiosulfonate afforded the spirocycle **3z** in 82% yield with excellent chemoselectivity. Selenosulfonylation was also possible using Se-phenyl benzenesulfonoselenoate with high selectivity. The structure of the major diastereomer of **3aa** was unambiguously determined by X-ray analysis (CCDC 2259733). Interelement compounds that simultaneously create carbon-sulfur and carbon–halogen atom bonds could also be utilized in the reaction (products **3ab** and **3ac**).[9r] Surprisingly, the reaction of BCB allyl esters with Se-phenyl benzenesulfonoselenoate didn't afford the desired cyclized product; instead, it gave direct addition product **3′** in 90% yield. The reaction with *gem*-dimethyl substituted BCB allyl ester **1b** was also unsuccessful.

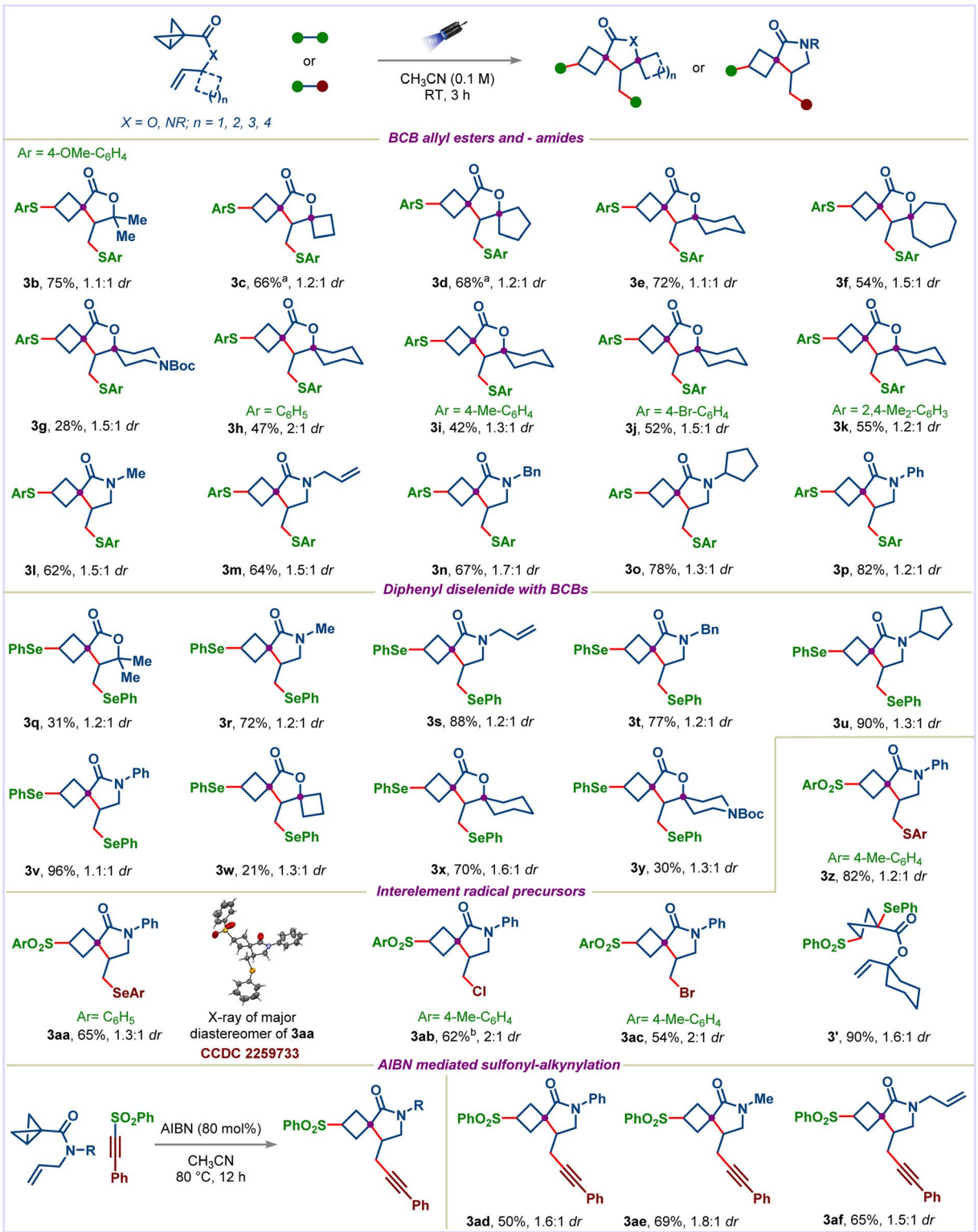

Scheme 3 Scope of BCB allyl esters and – amides with interelement compounds. Reaction conditions: 0.3 mmol of **1**, 0.3 mmol of interelement compound **2**, 3.0 mL of dry CH_3CN, 457 nm photocube, RT, 3 h. Yields are of isolated products and dr was determined by ^{1}H-NMR from the crude reaction mixture. [a] 0.2 mmol scale. [b] Using 365 nm.

Alkynes are versatile functional groups in organic synthesis. Introducing an alkyne group to spirocycles could enhance the transformability of these products. To our delight, treatment of **1l** with ((phenylethynyl)sulfonyl)benzene in the presence of AIBN under heating conditions provided the corresponding alkyne bearing spirocycle **3ad** in 50% yield.[20] Various

substituents on the nitrogen of BCB allyl amides were also well tolerated in this reaction (products **3ae** and **3af**).

Recently, dual photoredox/nickel catalysis has emerged as a powerful synthetic tool in organic chemistry for cross-coupling reactions of alkyl radicals with various electrophiles.[21] In most of these cross-coupling reactions, alkyl radicals can either be generated directly by homolytic cleavage of the C(sp^3)–X bond of a radical precursor or the generated radicals further undergo a cyclization, β-scission, migratory insertion, or 1,5-HAT process to give new radicals that take part in the following nickel catalyzed cross-coupling reaction. However, to the best of our knowledge, the dual photoredox/nickel strategy has never been applied to cross-coupling alkyl radicals resulting from the strain-enabled radical cascade. Realizing this would significantly extend our strategy to a three-component conjunctive cross-coupling reaction, thus allowing modular construction of diverse and complex spirocyclic scaffolds using readily available aryl sulfinates and (hetero)aryl or alkenyl halides.

Our studies began with the reaction of BCB allyl amide **1l**, sodium benzenesulfinate (**10a**), and 4-bromobenzonitrile (**11a**) (Fig. 2). Using 2.5 mol% of the organic photocatalyst (4CzIPN), 10 mol% $NiCl_2$·glyme and 15 mol% 4,4′-di-*tert*-butyl-2,2′-dipyridyl (**L_1**) in CH_3CN under blue light irradiation, the desired conjunctive cross-coupled product **12a** was obtained in 10% yield (Fig. 2, column 1). Changing to Lewis basic solvents, such as DMSO and DMA, the yield of the product **12a** was improved significantly (Fig. 2, columns 2 and 3). Other solvents were also examined but did not give any further improvement (see the ESI† for complete optimization). The yield could be improved to 71% by decreasing the reaction concentration (Fig. 2, column 4). Various ligands on the nickel catalyst had a substantial effect on the reaction yield: 1,10-phenanthroline (**L_2**) and 2,2′:6′,2′′-terpyridine (**L_3**) gave the desired product in much lower yields (Fig. 1, columns 5 and 6), whereas 2,2′-bipyridine (**L_4**) gave similar yield to dtbpy (Fig. 2, column 7). Among the photocatalysts tested, 4CzIPN emerged as the best catalyst (Fig. 2, columns 8–10). Finally, control experiments highlighted the necessity for the nickel catalyst, ligand, photocatalyst, and light (Fig. 2, columns 11–14).

With optimum conditions in hand, we first investigated the scope of the reaction with respect to BCB allyl amides (Scheme 4). Various substituents on the nitrogen, including simple phenyl, allyl, benzyl, and cyclopentyl groups were well tolerated (products **12a–12d**). Next, we explored a diverse range of aryl halides. Simple iodobenzene, electron-deficient, and electron-rich aryl halides could be successfully coupled to furnish the desired spirocycles **12e–12j** in moderate to good yields. The structure of the major diastereomer of **12i** was determined by X-ray analysis (CCDC 2292233). Coupling with 1-bromonapthalene was also possible, providing **12k** in 65% yield. Noteworthily, the use of heteroaryl halides allowed the introduction of heterocycles, such as quinoline and indole (products **12l** and **12m**). Next, we showed that alkenyl halides were also viable coupling partners in this reaction, providing the desired alkenylated products **12n** and **12o** in 37% and 67% yields, respectively. Finally, we explored the scope of aryl sulfinates: electron-donating and -withdrawing groups were well tolerated on the aryl ring (products **12p** and **12q**). Unfortunately, BCB allyl esters didn't give the desired products under photoredox/nickel dual catalysis.

To highlight the potential application of our method for the preparation of diverse spirocycles, several transformations of the obtained products were performed. We first synthesized the two spirocycles **3aa** and **3ac** on a 2 mmol scale with 70% and 50% yields, respectively (Scheme 5A). The phenylselenyl group was selectively reduced under radical conditions, giving spirocycle **13** in 79% yield (Scheme 5B). Oxidation followed by the

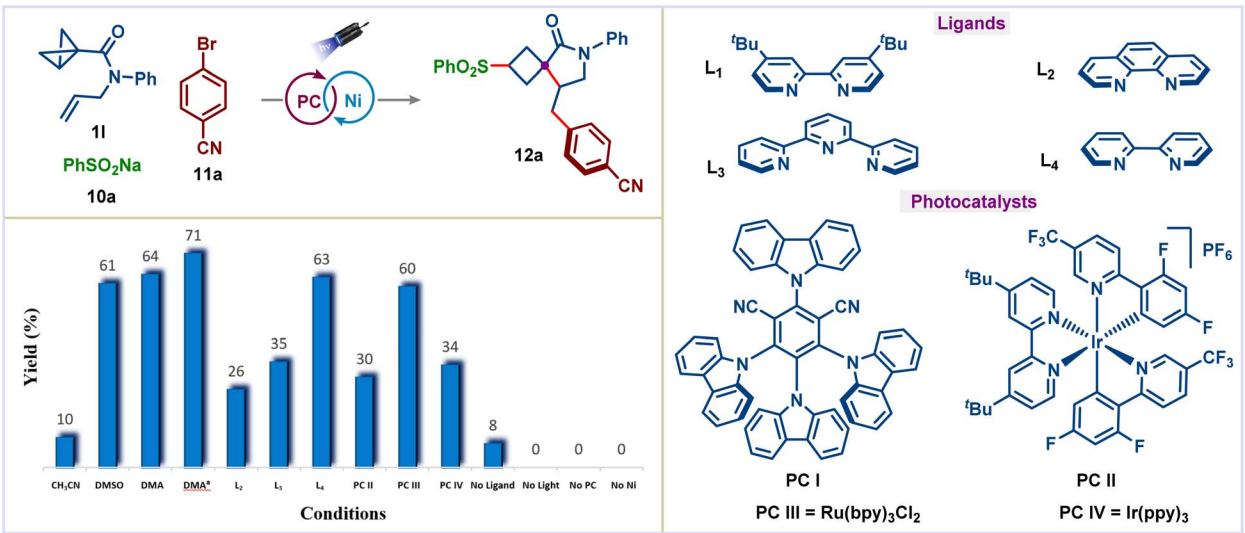

Fig. 2 Optimization of dual photoredox/nickel catalysis. Reactions were carried out under an inert atmosphere. Reaction conditions: **1l** (0.15 mmol, 1.0 equiv.), sodium benzenesulfinate (**10a**) (0.225 mmol, 1.5 equiv.), 4-bromobenzonitrile (**11a**) (0.30 mmol, 2.0 equiv.) and 4CzIPN (2.5 mol%), $NiCl_2$·glyme (10 mol%), L (15 mol%), 1.5 mL of solvent, 457 nm photocube, RT, 12 h. [a] 3.0 mL of DMA. Yields were determined by ^{1}H-NMR using CH_2Br_2 as the internal standard. In all cases, dr is ~2 : 1, which was determined by ^{1}H-NMR from the crude reaction mixture.

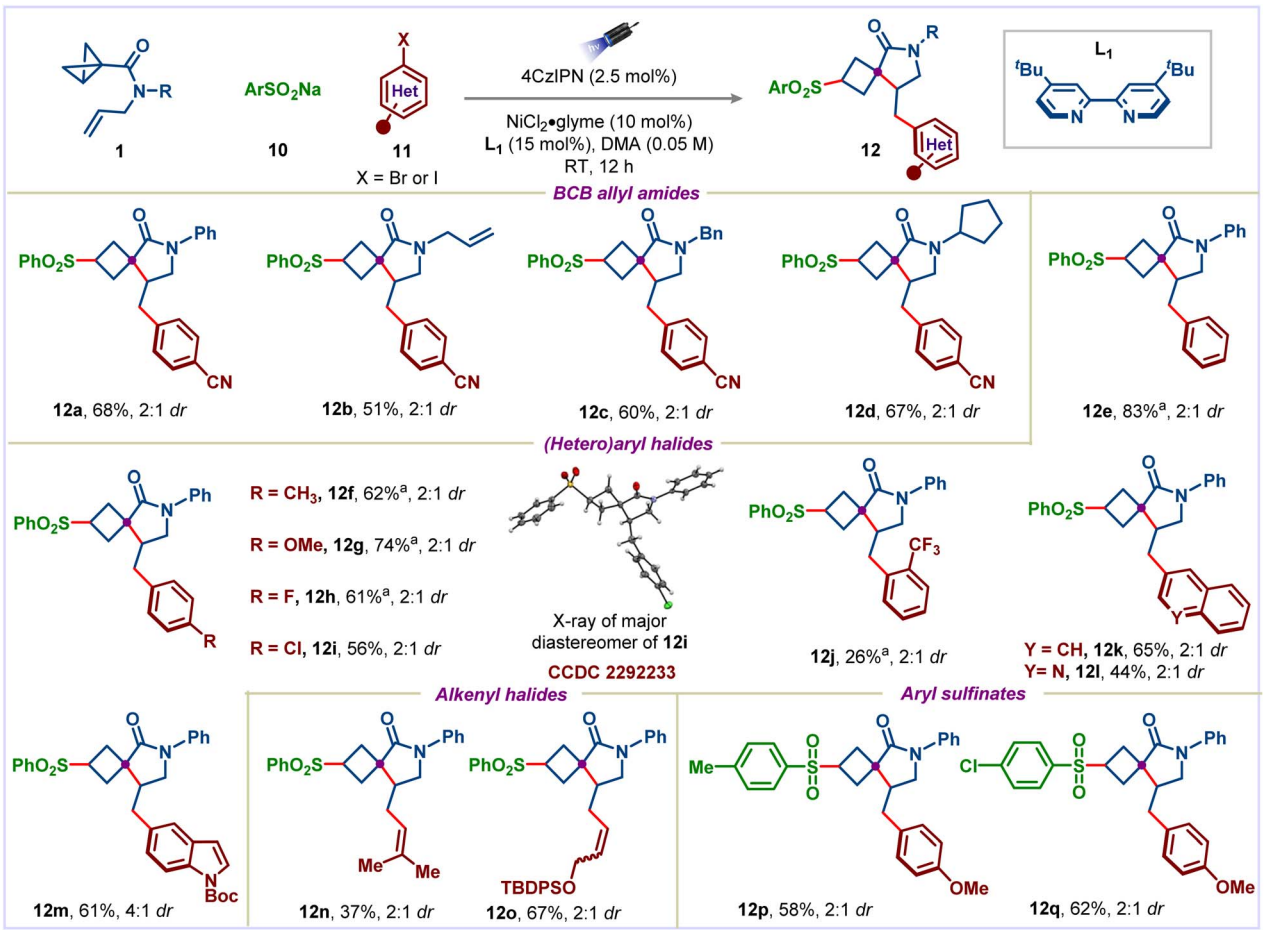

Scheme 4 Scope of dual photoredox/nickel catalysis. Reaction conditions: BCB **1** (0.30 mmol, 1.0 equiv.), sodium arylsulfinate **10** (0.45 mmol, 1.5 equiv.), (hetero)aryl or alkenyl halide **11** (0.60 mmol, 2.0 equiv.) and 4CzIPN (2.5 mol%), $NiCl_2$·glyme (10 mol%), L_1 (15 mol%), 6.0 mL of dry DMA, 457 nm photocube, RT, 12 h. Yields are of isolated products and dr was determined by ^{1}H-NMR from the crude reaction mixture. Unless otherwise mentioned, aryl-bromide was used. [a] Corresponding aryl-iodide was used.

Seleno-Cope reaction gave exocyclic double bond bearing spirocycle **14** in 41% yield. Treatment of **3aa** with borane gave spiro-pyrrolidine derivative **15**, a common motif present in several bioactive compounds.[22] Finally, we could introduce functional groups, which are highly challenging to install directly during the cascade. For example, we could displace

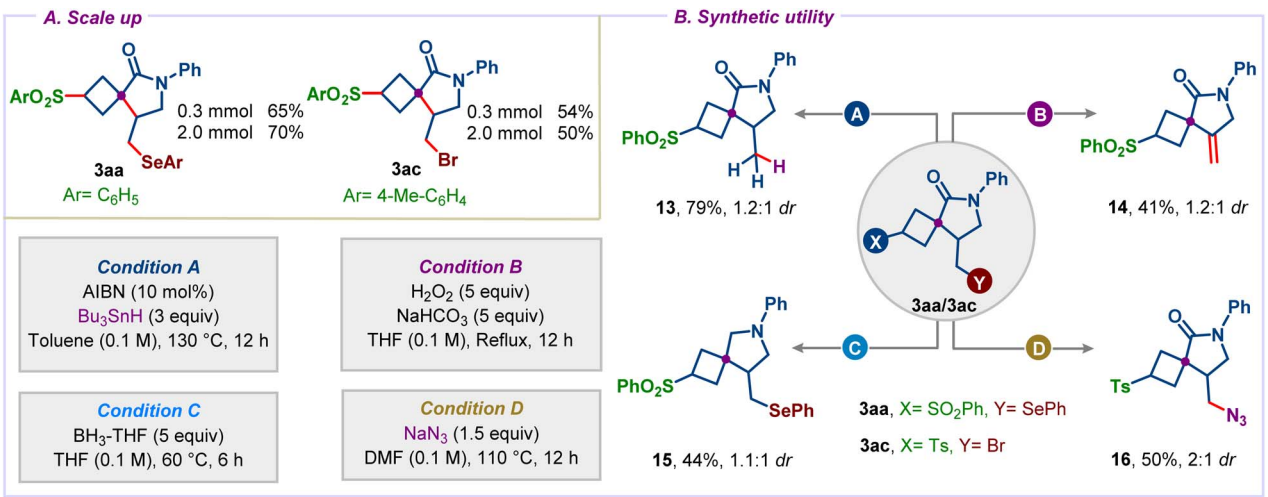

Scheme 5 (A) Scale up. (B) Synthetic utility.

bromide in **3ac** successfully with azide under heating conditions in DMF to access azide appended spirocycle **16** in 50% yield.

Next, we shed light on the mechanism of the reaction involving interelement compounds. To identify key reactive intermediates in this reaction, radical trapping experiments

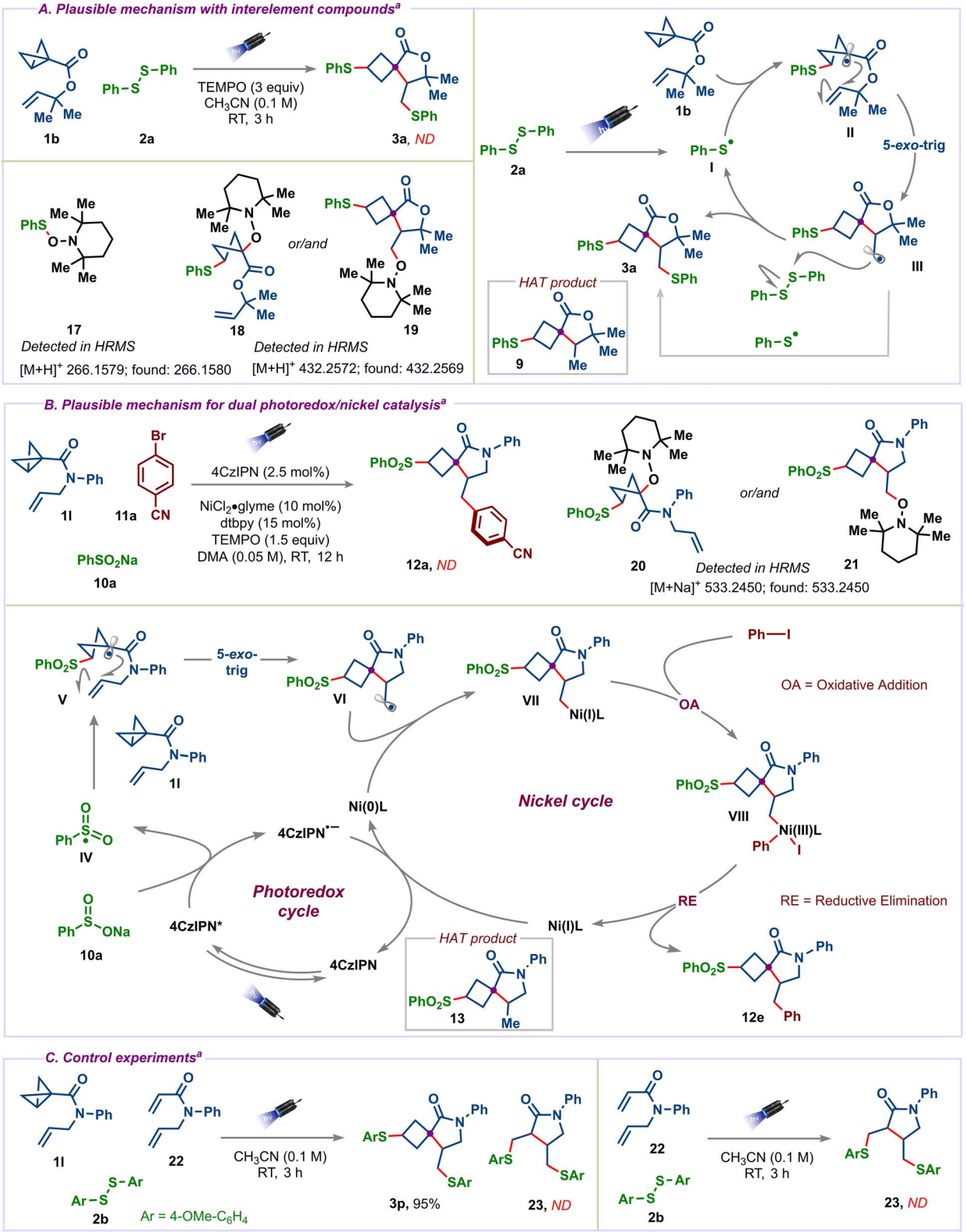

Scheme 6 (A) Plausible mechanism with interelement compounds. (B) Plausible mechanism for dual photoredox/nickel catalysis. (C) Control experiments. [a] Reactions were carried out on a 0.15 mmol scale. Light source: 457 nm photocube.

were performed (Scheme 6A). Adding 3 equiv. of TEMPO to the standard conditions led to the complete inhibition of product **3a**, with the detection of TEMPO adducts **17**, **18** and/or **19**. The identified compounds suggest that the reaction proceeds *via* a radical pathway. Based on radical trapping and literature reports,[18b,c] we proposed a plausible mechanism for this reaction. The homolytic cleavage of PhSSPh (**2a**) under visible light irradiation[23] leads to the thiyl radical **I**, which adds to the strained carbon–carbon bond of the BCB **1b** to give tertiary radical intermediate **II**. Subsequent 5-*exo*-trig cyclization of **II** generates primary alkyl radical **III**. Finally, intermediate **III** reacts with PhSSPh, affords the desired product, and regenerates the thiyl radical **I**. Alternatively, intermediate **III** combines with the thiyl radical **I** to give the desired product **3a.** The light on/off experiments suggest that light irradiation is needed throughout the reaction (see the ESI†). However, we cannot rule out the chain propagation mechanism at this stage. The detection of HAT product **9** indicates that the thiyl radical **I** first added to the strained carbon–carbon bond.

For the dual photoredox/nickel catalyzed conjunctive cross-coupling reaction, the mechanism starts with the reductive quenching of an excited state of the photocatalyst (PC = 4CzIPN) by single-electron-transfer (SET) from sodium-benzenesulfinate **10** to generate the sulfonyl radical **IV** ($E_{1/2}(PhO_2S^{\bullet}/PhSO_2Na) = -0.37$ V *vs.* SCE)[24] and ($E_{1/2}(PC^*/PC^{\bullet-}) = +1.43$ V *vs.* SCE)[25] (Scheme 6B). The addition of the sulfonyl radical to the strained carbon–carbon bond of the BCB **1l** then produces a tertiary radical **V**. Subsequent 5-*exo*-trig cyclization of the radical onto the olefin gives alkyl radical intermediate **VI**, which is quickly captured by the Ni(0) complex to furnish Ni(I) species **VII**. Oxidative addition of iodobenzene to the Ni(I) complex gives Ni(III) complex **VIII** that subsequently undergoes reductive elimination to give the desired product **12e** and Ni(I) species. Next, the reduction of Ni(I) by the reduced photocatalyst ($E_{1/2}(PC/PC^{\bullet-}) = -1.24$ V *vs.* SCE)[25a] regenerates the photocatalyst and Ni(0) species (Ni(I)/Ni(0) = −1.17 V *vs.* SCE)[26] to close both the catalytic cycles. The detection of TEMPO adducts **20** and/or **21** and HAT product **13** confirms the radical intermediacy in dual catalysis. Finally, successful control experiments (Scheme 6C) using *N*-allyl-*N*-phenylacrylamide[27] (**22**) under standard conditions with and without BCB **1l** showed that the lack of reactivity with **22** is due to the absence of strained bicyclobutane, which highlights the importance of ring-strain in enabling the present spirocyclization cascades.

Conclusion

In summary, we have developed the first strain-enabled radical spirocyclization cascade for the synthesis of functionalized spirocyclobutyl lactones and – lactams. The applicability of this strategy was further highlighted through the synthesis of a diverse family of bis-spirocyclic scaffolds. The reaction displays broad scope toward BCB allyl esters and – amides and diaryl disulfides with a wide range of functional group tolerance. The reaction was also successfully extended to the synthesis of selenium-substituted spirocycles. Furthermore, various interelement compounds reacted well in this reaction, giving spirocycles with multi-functional groups. Finally, dual photoredox/nickel catalyzed conjunctive cross-coupling of BCB allyl amides with aryl sulfinates and (hetero)aryl halides has been developed for the synthesis of arylated spirocyclobutyl lactams. The multiple points for diversifying the obtained spirocycles provided the potential to construct medicinally relevant spirocycles rapidly. Further extending this methodology to other radical precursors and their applications is currently under investigation in our laboratory.

Data availability

General information, experimental procedures, characterization data for all new compounds, and NMR spectra are in the ESI.† Data for the crystal structure reported in this paper have been deposited at the Cambridge Crystallographic Data Centre (CCDC) under the deposition number CCDC 2259733 and 2292233.

Author contributions

K. D. and D. P. H. conceived and designed the project. K. D. carried out optimization studies, substrate scope, and mechanistic studies. A. P. and T. S. helped in the substrate scope studies. D. P. H. and K. D. wrote the manuscript with suggestions from A. P. and T. S. All authors have given approval to the final version of the manuscript.

Conflicts of interest

There are no conflicts to declare.

Acknowledgements

Financial support from the Science and Engineering Research Board (SERB), Government of India (File CRG/2022/007372), is greatly acknowledged. D. P. H. thanks the Indian Institute of Science (IISc) Bangalore for the infrastructure. T. S. thanks the Ministry of Education, Government of India for PMRF.

Notes and references

1 (*a*) E. M. Carreira and T. C. Fessard, *Chem. Rev.*, 2014, **114**, 8257–8322; (*b*) Y.-J. Zheng and C. M. Tice, *Expert Opin. Drug Discovery*, 2016, **11**, 831–834; (*c*) A. J. Boddy and J. A. Bull, *Org. Chem. Front.*, 2021, **8**, 1026–1084; (*d*) K. Hiesinger, D. Dar'in, E. Proschak and M. Krasavin, *J. Med. Chem.*, 2021, **64**, 150–183; (*e*) N. Moshnenko, A. Kazantsev, E. Chupakhin, O. Bakulina and D. Dar'in, Synthetic Routes to Approved Drugs Containing a Spirocycle, *Molecules*, 2023, **28**, 4209.
2 K. E. Prosser, R. W. Stokes and S. M. Cohen, *ACS Med. Chem. Lett.*, 2020, **11**, 1292–1298.
3 (*a*) D. E. Rathkopf and H. I. Scher, *Expert Rev. Anticancer Ther.*, 2018, **18**, 823–836; (*b*) M. A. Rice, S. V. Malhotra and T. Stoyanova, *Front. Oncol.*, 2019, **9**, 801; (*c*) M. R. van der

Kolk, M. A. C. H. Janssen, F. P. J. T. Rutjes and D. Blanco-Ania, *ChemMedChem*, 2022, **17**, e202200020.

4 Y. Zheng, C. M. Tice and S. B. Singh, *Bioorg. Med. Chem. Lett.*, 2014, **24**, 3673–3682.

5 Selected patents on spirocyclobutyl lactones:(*a*) D. J. Canney, B. E. Blass, R. Gao and M. Abou-Gharbia, Novel 5-Hydroxytryptamine Receptor 7 Activity Modulators and Their Method of Use, WO2016040554A1, 2016; (*b*) D. J. Canney, B. E. Blass, R. Gao and K. Blattner, Novel Sigma-2 Receptor Binders and Their Method of Use, WO2016183150A1, 2016; (*c*) S. Angle, J. Cao, J. Come, L. A. Dakin, Z. Gale-Day, E. B. Krueger, J. H. Olsen, T. J. Senter, A. J. Shimizu, S. D. Stone and T. Wang, 2-Methyl-4′,5′-Dihydrospiro[Piperidine-4,7′-Thieno[2,3-C] Pyran] Derivatives as Inhibitors of Apol1 and Methods of Using Same, WO2023154344A1, 2023, selected patents on spirocyclobutyl lactams; (*d*) J. Caravella, B. Han, C. Liu, S. Ioannidis, A. J. Buckmelter, D. J. Richard, M. W. Martin, S. Mischke and S. Mente, Inhibiting Ubiquitin Specific Peptidase 30, EP3692028A1, 2020; (*e*) F. Jakob, J. Alen, S. Krüger, D. Friebe, S. Hennen and P. Barbie, Substituted Pyrrolidine Amides III, US2022089573A1, 2022; (*f*) S. Liu, Z. Yu, W. Pang, J. Wang and P. Chen, Highly Active CSF1R Inhibitor Compound, US11591328B2, 2023.

6 (*a*) M. Bertrand, A. Meou and A. Tubul, *Tetrahedron Lett.*, 1982, **23**, 3691–3694; (*b*) A. Call, M. Cianfanelli, P. Besalú-Sala, G. Olivo, A. Palone, L. Vicens, X. Ribas, J. M. Luis, M. Bietti and M. Costas, *J. Am. Chem. Soc.*, 2022, **144**, 19542–19558; (*c*) Z. Zhang and V. Gevorgyan, *J. Am. Chem. Soc.*, 2022, **144**, 20875–20883.

7 (*a*) J. Turkowska, J. Durka and D. Gryko, *Chem. Commun.*, 2020, **56**, 5718–5734; (*b*) J. L. Tyler and V. K. Aggarwal, *Chem.–Eur. J.*, 2023, **29**, e202300008; (*c*) C. B. Kelly, J. A. Milligan, L. J. Tilley and T. M. Sodano, *Chem. Sci.*, 2022, **13**, 11721–11737; (*d*) P. Bellotti and F. Glorius, *J. Am. Chem. Soc.*, 2023, **145**, 20716–20732.

8 (*a*) M. A. A. Walczak, T. Krainz and P. Wipf, *Acc. Chem. Res.*, 2015, **48**, 1149–1158; (*b*) M. Golfmann and J. C. L. Walker, *Commun. Chem.*, 2023, **6**, 9.

9 (*a*) Y. Gaoni, A. Tomazic and E. Potgieter, *J. Org. Chem.*, 1985, **50**, 2943–2947; (*b*) T. G. Archibald, L. C. Garver, K. Baum and M. C. Cohen, *J. Org. Chem.*, 1989, **54**, 2869–2873; (*c*) R. Gianatassio, J. M. Lopchuk, J. Wang, C.-M. Pan, L. R. Malins, L. Prieto, T. A. Brandt, M. R. Collins, G. M. Gallego, N. W. Sach, J. E. Spangler, H. Zhu, J. Zhu and P. S. Baran, *Science*, 2016, **351**, 241–246; (*d*) J. A. Milligan, C. A. Busacca, C. H. Senanayake and P. Wipf, *Org. Lett.*, 2016, **18**, 4300–4303; (*e*) J. M. Lopchuk, K. Fjelbye, Y. Kawamata, L. R. Malins, C.-M. Pan, R. Gianatassio, J. Wang, L. Prieto, J. Bradow, T. A. Brandt, M. R. Collins, J. Elleraas, J. Ewanicki, W. Farrell, O. O. Fadeyi, G. M. Gallego, J. J. Mousseau, R. Oliver, N. W. Sach, J. K. Smith, J. E. Spangler, H. Zhu, J. Zhu and P. S. Baran, *J. Am. Chem. Soc.*, 2017, **139**, 3209–3226; (*f*) X. Wu, W. Hao, K.-Y. Ye, B. Jiang, G. Pombar, Z. Song and S. Lin, *J. Am. Chem. Soc.*, 2018, **140**, 14836–14843; (*g*) A. Fawcett, T. Biberger and V. K. Aggarwal, *Nat. Chem.*, 2019, **11**, 117–122; (*h*) M. Silvi and V. K. Aggarwal, *J. Am. Chem. Soc.*, 2019, **141**, 9511–9515; (*i*) S. H. Bennett, A. Fawcett, E. H. Denton, T. Biberger, V. Fasano, N. Winter and V. K. Aggarwal, *J. Am. Chem. Soc.*, 2020, **142**, 16766–16775; (*j*) G. Ernouf, E. Chirkin, L. Rhyman, P. Ramasami and J.-C. Cintrat, *Angew. Chem., Int. Ed.*, 2020, **59**, 2618–2622; (*k*) M. Ociepa, A. J. Wierzba, J. Turkowska and D. Gryko, *J. Am. Chem. Soc.*, 2020, **142**, 5355–5361; (*l*) C. J. Pratt, R. A. Aycock, M. D. King and N. T. Jui, *Synlett*, 2020, **31**, 51–54; (*m*) B. D. Schwartz, M. Y. Zhang, R. H. Attard, M. G. Gardiner and L. R. Malins, *Chem.–Eur. J.*, 2020, **26**, 2808–2812; (*n*) X. Yu, M. Lübbesmeyer and A. Studer, *Angew. Chem., Int. Ed.*, 2021, **60**, 675–679; (*o*) G. Tan, M. Das, H. Keum, P. Bellotti, C. Daniliuc and F. Glorius, *Nat. Chem.*, 2022, **14**, 1174–1184; (*p*) J. Majhi, R. K. Dhungana, Á. Rentería-Gómez, M. Sharique, L. Li, W. Dong, O. Gutierrez and G. A. Molander, *J. Am. Chem. Soc.*, 2022, **144**, 15871–15878; (*q*) A. Guin, S. Bhattacharjee, M. S. Harariya and A. T. Biju, *Chem. Sci.*, 2023, **14**, 6585–6591; (*r*) H. D. Pickford, V. Ripenko, R. E. McNamee, S. Holovchuk, A. L. Thompson, R. C. Smith, P. K. Mykhailiuk and E. A. Anderson, *Angew. Chem., Int. Ed.*, 2023, **62**, e202213508; (*s*) W. Huang, Y. Zheng, S. Keess and G. A. Molander, *J. Am. Chem. Soc.*, 2023, **145**, 5363–5369; (*t*) H.-C. Shen, M. V. Popescu, Z.-S. Wang, L. de Lescure, A. Noble, R. S. Paton and V. K. Aggarwal, *J. Am. Chem. Soc.*, 2023, **145**, 16508–16516; (*u*) H. Wang, J. E. Erchinger, M. Lenz, S. Dutta, C. G. Daniliuc and F. Glorius, *J. Am. Chem. Soc.*, 2023, **145**, 23771–23780.

10 (*a*) R. M. Bychek, V. Hutskalova, Y. P. Bas, O. A. Zaporozhets, S. Zozulya, V. V. Levterov and P. K. Mykhailiuk, *J. Org. Chem.*, 2019, **84**, 15106–15117; (*b*) X. Ma, D. L. Sloman, Y. Han and D. J. Bennett, *Org. Lett.*, 2019, **21**, 7199–7203; (*c*) R. E. McNamee, M. M. Haugland, J. Nugent, R. Chan, K. E. Christensen and E. A. Anderson, *Chem. Sci.*, 2021, **12**, 7480–7485; (*d*) R. Bychek and P. K. Mykhailiuk, *Angew. Chem., Int. Ed.*, 2022, **61**, e202205103.

11 (*a*) M. Ueda, M. A. A. Walczak and P. Wipf, *Tetrahedron Lett.*, 2008, **49**, 5986–5989; (*b*) K. Dhake, K. J. Woelk, J. Becica, A. Un, S. E. Jenny and D. C. Leitch, *Angew. Chem., Int. Ed.*, 2022, **61**, e202204719; (*c*) Z. Ding, Z. Liu, Z. Wang, T. Yu, M. Xu, J. Wen, K. Yang, H. Zhang, L. Xu and P. Li, *J. Am. Chem. Soc.*, 2022, **144**, 8870–8882; (*d*) R. Guo, Y.-C. Chang, L. Herter, C. Salome, S. E. Braley, T. C. Fessard and M. K. Brown, *J. Am. Chem. Soc.*, 2022, **144**, 7988–7994; (*e*) R. Kleinmans, T. Pinkert, S. Dutta, T. O. Paulisch, H. Keum, C. G. Daniliuc and F. Glorius, *Nature*, 2022, **605**, 477–482; (*f*) Y. Liang, R. Kleinmans, C. G. Daniliuc and F. Glorius, *J. Am. Chem. Soc.*, 2022, **144**, 20207–20213; (*g*) B. D. Schwartz, A. P. Smyth, P. E. Nashar, M. G. Gardiner and L. R. Malins, *Org. Lett.*, 2022, **24**, 1268–1273; (*h*) Y. Zheng, W. Huang, R. K. Dhungana, A. Granados, S. Keess, M. Makvandi and G. A. Molander, *J. Am. Chem. Soc.*, 2022, **144**, 23685–23690; (*i*) S. Agasti, F. Beltran, E. Pye, N. Kaltsoyannis, G. E. M. Crisenza and D. J. Procter, *Nat. Chem.*, 2023, **15**, 535–541; (*j*) R. Kleinmans, S. Dutta, K. Ozols, H. Shao, F. Schäfer, R. E. Thielemann,

H. T. Chan, C. G. Daniliuc, K. N. Houk and F. Glorius, *J. Am. Chem. Soc.*, 2023, **145**, 12324–12332; (*k*) T. Yu, J. Yang, Z. Wang, Z. Ding, M. Xu, J. Wen, L. Xu and P. Li, *J. Am. Chem. Soc.*, 2023, **145**, 4304–4310; (*l*) Y. Liu, S. Lin, Y. Li, J.-H. Xue, Q. Li and H. Wang, *ACS Catal.*, 2023, **13**, 5096–5103; (*m*) N. Radhoff, C. G. Daniliuc and A. Studer, *Angew. Chem., Int. Ed.*, 2023, **62**, e202304771; (*n*) Y. Liang, F. Paulus, C. G. Daniliuc and F. Glorius, *Angew. Chem., Int. Ed.*, 2023, **62**, e202305043; (*o*) T. V. T. Nguyen, A. Bossonnet, M. D. Wodrich and J. Waser, *J. Am. Chem. Soc.*, 2023, **145**, 25411–25421.

12 N. A. Meanwell, *J. Agric. Food Chem.*, 2023, **71**, 18087–18122.

13 S. Stotani, C. Lorenz, M. Winkler, F. Medda, E. Picazo, R. Ortega Martinez, A. Karawajczyk, J. Sanchez-Quesada and F. Giordanetto, *ACS Comb. Sci.*, 2016, **18**, 330–336.

14 G. Tan, F. Paulus, A. Petti, M.-A. Wiethoff, A. Lauer, C. Daniliuc and F. Glorius, *Chem. Sci.*, 2023, **14**, 2447–2454.

15 Y. Lu, C. Chen, H. Zhu, Z. Luo and Y. Zhang, *Green Chem.*, 2022, **24**, 8021–8028.

16 V. A. Vasin, A. V. Semenov, S. G. Kostryukov and V. V. Razin, *Russ. J. Org. Chem.*, 2008, **44**, 1296–1304.

17 E. D. Hughes and C. K. Ingold, *J. Chem. Soc.*, 1935, 244–255.

18 (*a*) M. Teders, C. Henkel, L. Anhäuser, F. Strieth-Kalthoff, A. Gómez-Suárez, R. Kleinmans, A. Kahnt, A. Rentmeister, D. Guldi and F. Glorius, *Nat. Chem.*, 2018, **10**, 981–988; (*b*) R. M. Bär, G. Heinrich, M. Nieger, O. Fuhr and S. Bräse, *Beilstein J. Org. Chem.*, 2019, **15**, 1172–1180; (*c*) C. Wang, Y. Zhang, K. Sun, T. Yu, F. Liu and X. Wang, *Molecules*, 2023, **28**, 1–35.

19 H. Chuai, S.-Q. Zhang, H. Bai, J. Li, Y. Wang, J. Sun, E. Wen, J. Zhang and M. Xin, *Eur. J. Med. Chem.*, 2021, **223**, 113621.

20 (*a*) J. Gong and P. L. Fuchs, *J. Am. Chem. Soc.*, 1996, **118**, 4486–4487; (*b*) L. Liang, G. Guo, C. Li, S.-L. Wang, Y.-H. Wang, H.-M. Guo and H.-Y. Niu, *Org. Lett.*, 2021, **23**, 8575–8579.

21 (*a*) C. Zhu, H. Yue, L. Chu and M. Rueping, *Chem. Sci.*, 2020, **11**, 4051–4064; (*b*) S. O. Badir and G. A. Molander, *Chem*, 2020, **6**, 1327–1339; (*c*) M. Marchi, G. Gentile, C. Rosso, M. Melchionna, P. Fornasiero, G. Filippini and M. Prato, *ChemSusChem*, 2022, **15**, e202201094; (*d*) Z. Zuo, D. T. Ahneman, L. Chu, J. A. Terrett, A. G. Doyle and D. W. C. MacMillan, *Science*, 2014, **345**, 437–440; (*e*) E. B. Corcoran, M. T. Pirnot, S. Lin, S. D. Dreher, D. A. DiRocco, I. W. Davies, S. L. Buchwald and D. W. C. MacMillan, *Science*, 2016, **353**, 279–283; (*f*) X. Zhang, R. T. Smith, C. Le, S. J. McCarver, B. T. Shireman, N. I. Carruthers and D. W. C. MacMillan, *Nature*, 2020, **580**, 220–226; (*g*) Z. Dong and D. W. C. MacMillan, *Nature*, 2021, **598**, 451–456; (*h*) C. N. Prieto Kullmer, J. A. Kautzky, S. W. Krska, T. Nowak, S. D. Dreher and D. W. C. MacMillan, *Science*, 2022, **376**, 532–539.

22 (*a*) S. Hoelder, J. Blagg, S. Solanki, H. Woodward, S. Naud, V. Bavetsias, P. Sheldrake, P. Innocenti, J. Cheung and B. Atrash, Inhibitor Compounds, WO2014037750A1, 2014; (*b*) G. A. Brown, J. E. Cansfield, M. S. Congreve, M. A. O'brien, M. Pickworth, M. D. Rackham, B. G. Tehan and B. J. Teobold, Bicyclic Aza Compounds as Muscarinic M1 Receptor Agonists, WO2015118342A1, 2015; (*c*) F. Wagner and D. Hickman, Hdac6 Inhibitors and Uses Thereof, WO2023150203A1, 2023.

23 (*a*) H. Ruan, L.-G. Meng, L. Zhu and L. Wang, *Adv. Synth. Catal.*, 2019, **361**, 3217–3222; (*b*) S.-Y. Tian, J.-J. Ai, J.-H. Han, W. Rao, S.-S. Shen, D. Sheng and S.-Y. Wang, *J. Org. Chem.*, 2023, **88**, 828–837.

24 A. U. Meyer, S. Jäger, D. Prasad Hari and B. König, *Adv. Synth. Catal.*, 2015, **357**, 2050–2054.

25 (*a*) E. Speckmeier, T. G. Fischer and K. Zeitler, *J. Am. Chem. Soc.*, 2018, **140**, 15353–15365; (*b*) X. Du, I. Cheng-Sánchez and C. Nevado, *J. Am. Chem. Soc.*, 2023, **145**, 12532–12540.

26 S. H. Lau, M. A. Borden, T. J. Steiman, L. S. Wang, M. Parasram and A. G. Doyle, *J. Am. Chem. Soc.*, 2021, **143**, 15873–15881.

27 (*a*) I. De Riggi, S. Gastaldi, J. M. Surzur, M. P. Bertrand and A. Virgili, *J. Org. Chem.*, 1992, **57**, 6118–6125; (*b*) T. Naito, Y. Honda, O. Miyata and I. Ninomiya, *J. Chem. Soc., Perkin Trans. 1*, 1995, 19–26.